Comparison of Soot-foil and Velocity Map Measurements in Gaseous Detonations

Delbert R. Hart, Liliana L. Berson, Rachel Hytovick, Kareem A. Ahmed
Center for Advanced Turbomachinery and Energy Research, Department of Mechanical and Aerospace Engineering, University of Central Florida
Orlando, Florida, United States

1 Abstract

Cellular structures are a prominent aspect of gaseous detonations. These structures have been used to characterize detonations with parameters such as cell widths, which have been successfully correlated to the mixture of the detonation, among other characteristics. Traditionally, soot-foils have been used to identify cell structures, with more recent advances in imaging technology making shadowgraph imaging able to also identify cell structures. To date, these methods have been regarded as two distinct processes. Soot-foils collect time-integrated cellular structures, while shadowgraph imaging collects transient structures in the detonation. Through further processing of the shadowgraph data, parameters such as front velocity and temperature can be found. From these parameters a velocity map can be constructed, which reveals cellular structures that are the same as soot-foils. A series of experiments were run in the National Automated Detonation Facility at the University of Central Florida of stoichiometric mixtures of methane and oxygen with varying levels of nitrogen dilution. The cellular structures were collected via three different methods: analyzing cell structure in soot-foils, tracking triple points through shadowgraph data, and analyzing the cell structure in velocity maps. This paper aims to unify the measurements collected from soot-foils and velocity maps and presents a method that contains more information than soot-foils.

2 Introduction

As 2-dimensional detonations travel through time and space, triple points move along the detonation front, and occasionally cross each other. By integrating the path of the triple points, they create cells that vary in shape and size depending on the detonation mixtures. Since the 1900's these cells have been used to described characteristics of detonations. Traditionally, cells have been measured with soot-foils, and have been described using shadowgraph imaging only recently. To measure cells with soot-foils, sooted steel sheets would be placed on the side or end walls of a facility to capture the cell structure as the detonation front passes over the sheets or hits the wall [1], [2]. This creates time-integrated data related to the detonation. Early cell structure studies have described the detonability of gaseous detonations [3]. Since then, the cell width has since been related to the induction zone [3] and has been

Correspondence to: delbert.hart@ucf.edu

attempted to be used to obtain other detonation characteristics, such as the critical tube diameter [4], which is currently an ongoing issue. To extract useful information from the cellular structures, significant setup and post processing is required. This includes coating a metal sheet with soot, imaging the cell structure and detecting cell edges. After post processing is complete, the cell width can be quantified, and the cell regularity can also be described. However, in detonations with irregular cells, the cell widths and lengths vary, making it difficult to describe a characteristic length like cell widths. Detonations with high nitrogen concentrations tend to have both irregular cell structure and large cell widths. Akbar et al. documented cell sizes in the Detonation Database [5], including data of cell width evolution in stoichiometric methane-oxygen mixtures with varying nitrogen dilutions.

As the framerates of cameras have increased, shadowgraph imaging has become widely used in detonation research. From shadowgraph images, transient structures can be seen in the detonation front, including Mach stems, transverse waves, incident shocks, and unburnt gas pockets. By combining frame-by-frame shots of the detonation front, the front's velocity can be found. By creating a velocity map, cellular structures appear [6], [7]. From these velocity maps, information such as the temperature, pressure, and density can be calculated [8]. Significant set-up and post processing must be taken to extract the data, including setting up diagnostics and processing the images.

While the exact process of how soot-foils are created on steel sheets is still unknown, it is accepted that the soot is deposited at the location of the triple points (the intersection of Mach stems, transverse waves, and incident shocks), and the cellular structure is created due to triple points travelling through time [9].

Carter et al. [10] posited that either schlieren or soot-foils could be used to obtain data on the detonation front. This paper aims to build on that, and to further posit that the data obtained from shadowgraph can replicate the cellular data obtained from soot-foils. While soot-foils can only collect time-integrated data that can describe the cell structure, shadowgraph can accurately collect data on cell structure, velocity and detonation front characteristics, such as Mach stems, incident shocks, transverse waves, and unburnt gas pockets. The additional velocity data allows for the calculation of density, pressure, and temperature of the post-shock conditions. Data from stoichiometric methane-oxygen mixtures with varying levels of nitrogen dilution will be analyzed, with cell widths being compared between velocity maps, soot-foils, and triple point tracks through time.

3 Methodology

Experiments were conducted in the National Automation Detonation Facility (NADF). The facility is a 3.6-meter tube with a cross section of 25-mm x 100-mm. The facility contains a converging section that reduces the cross section to 2-mm x 100-mm, which allows for nominally 2D detonation waves to be studied. This 2D approximation introduces significant wall effects, which limits the use of shadowgraph data collected to that of detonations with high wall effects. The facility has five distinct parts: a dual predetonator, a driver section, a converging section, a test section, and a damping section. The process is initiated with a sparkplug in the predetonator section, which travels down two 450-mm Shchelkin tubes. The flame arrives at the driver section where it is allowed to reach a planar state, then will encounter perforated plates which will initiate the deflagration to detonation transition (DDT), where the flame then becomes a detonation. The detonation reaches the converging section, which reduces the flow to a 2-mm wide channel. The detonation then passes through a straight 46-cm section to further allow the detonation to stabilize after the contraction. The detonation reaches the test section and passes to the damping section where the detonation then is dispersed. The facility is fully automated, and can handle gas injection (diluent, fuel, oxidizer), ignition, purge, and data collection.

A mixture of stoichiometric methane-oxygen was used for all tests, with varying degrees of nitrogen dilution, as seen in Table 1. The detonations in this study were irregular due to their high activation

energy. As the cell widths continue to increase due to increased nitrogen dilution, the detonations should be considered at near limit.

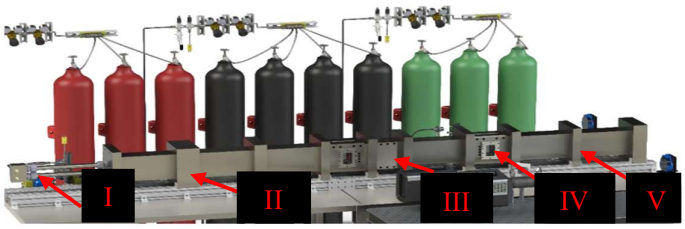

Figure 1: The National Automated Detonation Facility. From left to right: I. the predetonator, II. the driver section, III. the converging section, IV. the test section, and V. the damping flange.

To capture the shadowgraph data, a Hadlands Shimadzu HPV-X2 camera was used with a 640-nm CAVILUX Smart UHS system as the light source. The image size was 250 x 400 pixels, with varying levels of image resolution, as shown in Table 1. The Shimadzu took 256 images throughout the detonation and is triggered by a pressure transducer positioned before the test section. Therefore, images of the test section were captured before and after the detonation passed through. The triple point tracks (TPT) were determined by annotating the positions of the triple points by hand through each frame of the detonation. A video editing software was used to mark the points of the triple points frame-by-frame, then the triple points were extracted from the software and plotted. The velocity map was created by capturing instantaneous data of the detonation front through time and was plotted on a color map [8]. To capture soot-foil data, the quartz glass window was sooted before the detonation, and the initial image was subtracted from the final image using a subtraction method described by Hargather & Settles [11], which became the soot-foil. This was annotated by hand to identify the cell structure in the soot-foil.

Table 1: List of test conditions and important parameters in the stoichiometric methane-oxygen mixture.

Chemical Formula	Pixel Resolution (μm / px)	CJ Velocity (m/s)	Window Height (mm)	Window Length (mm)	Channel Thickness to Cell Width Ratio
$0.5CH_4 + O_2$	69.6	2390.8	27.9	17.4	2.62
$0.5CH_4 + O_2 + 0.11N_2$	70.0	2348.1	28.0	17.5	2.36
$0.5CH_4 + O_2 + 0.2N_2$	79.7	2301.1	31.9	19.9	1.72
$0.5CH_4 + O_2 + 0.67N_2$	117.9	2190.0	47.0	29.4	-
$0.5CH_4 + O_2 + 1.5N_2$	115.7	2041.6	46.3	28.9	-

A total of 17 cell widths were measured across 11 different tests using each of the measurement methods (soot-foil, TPT, and velocity map). For a given test, a cell width was measured only if that cell width was identifiable by each measurement method. The triple point track measurements were assumed to be the true values, since the cell width data from the TPT can be extracted directly from raw footage. Therefore, the soot-foil and velocity map cell widths' error are recorded with respect to the TPT cell widths. The standard deviation of the measurements was reported and the mean cell sizes of the TPT were compared against the Detonation Database compiled by Caltech for varying nitrogen dilution of a stoichiometric methane-oxygen mixture at 102 kPa and 293 K. Randomly deleting half of the dataset showed that the error values for the differences of cell width between the TPT and other two measurements showed statistical convergence. Additionally, the mean values of the different measurement methods statistically converge for the 0 %, 10 %, and 20 % nitrogen dilution cases. As

noted later, the cell widths of the 40 % and 60 % nitrogen dilution cases were unable to be accurately measured.

4 Results

By hand plotting the triple points through time, a map of the triple point evolution was created, which revealed cell structures. Additionally, by hand annotating the soot-foils and velocity maps, cell structures were able to be obtained. From these structures the cell width was extracted, which is the metric of comparison in this study. When evaluating the error of the velocity map cell widths and soot-foil cell widths, the triple point track cell widths were used as the true value.

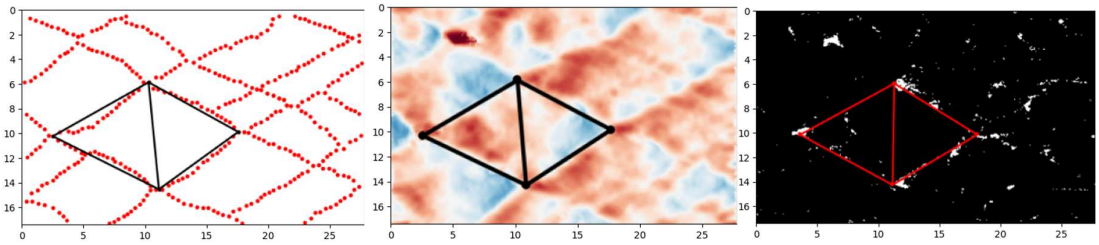

Figure 4: From left to right: The TPT, the velocity map, and soot-foil for a stoichiometric $0.5CH_4 + O_2$ case, in scale of millimeters.

The cell width's standard deviation across the three nitrogen dilution cases for all measurement methods was below 3.75 mm, with the soot-foil measurements having the lowest standard deviation. When calculating the error of the soot-foil cell widths and the velocity map cell widths with the TPT cell widths, it was shown both average errors across the nitrogen dilutions were less than 7.5 %, where the soot-foil's error was higher than the velocity map's error.

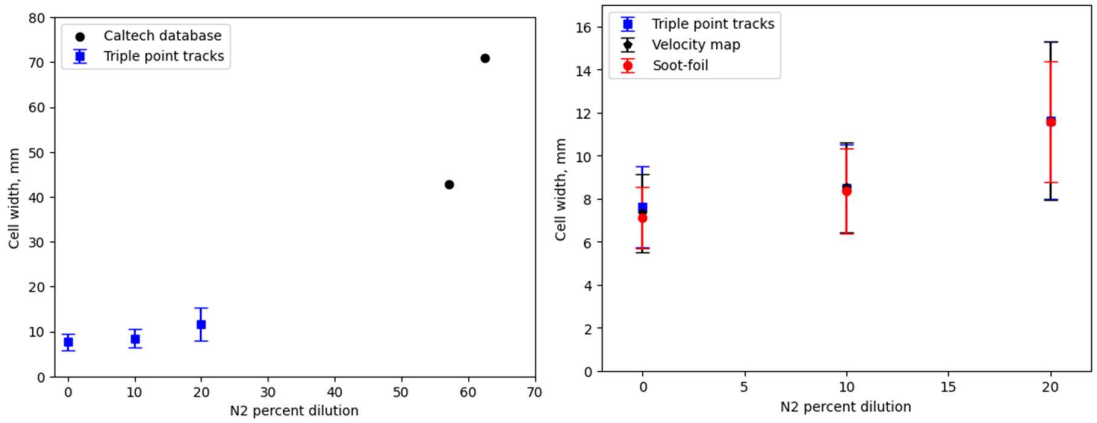

Figure 5: Left: TPT cell width plotted with the data from the Detonation Database. The collected data seems to fit with the data collected by Caltech. Right: The average cell width as the nitrogen dilution varies, as collected by different measurement methods.

Table 2: Error of the cell widths between the TPT and the two other cell width measurements for nitrogen dilutions of 0 %, 10 %, and 20 %, expressed as percentages.

Measurement's Error	0 % N_2 dilution (%)	10 % N_2 dilution (%)	20 % N_2 dilution (%)
Soot-foil | TPT	9.47	6.19	5.41
Velocity map | TPT	4.30	1.66	3.77

Comparing the mean magnitudes of the cell widths from the Detonation Database, there seems to be good agreement with the exponential trend that is shown in the database. From the collected data, as the nitrogen dilution increases in the mixture, the cell widths will also increase. The Detonation Database also shows that the cell width will increase with increasing nitrogen dilutions. As the cell width approaches and exceeds the viewing window's height, the cell structure would become increasingly harder to identify, as seen in the 40 % nitrogen dilution case. This caused cell width measurements for the 40 % and 60 % nitrogen dilution cases to be difficult to measure. However, visually inspecting the data reveals the TPT to match both the velocity map and the soot-foil.

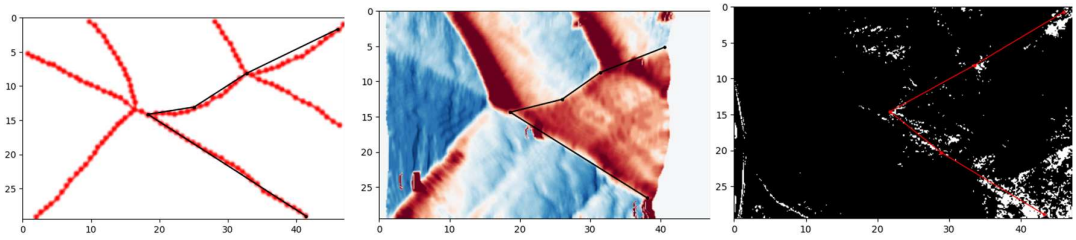

Figure 6: From left to right: The triple point tracks, the velocity map, and the soot-foil for a $0.5CH_4 + O_2 + 0.67N_2$ case, with the scale in millimeters. While the cell width is too large to be measured accurately, the features still align with each other.

5 Conclusion

Three different methods of measurement were used to collect data on cell structures: annotation of triple points from shadowgraph images, soot-foils on glass, and velocity maps created from detonation front analysis. The cell widths collected from the velocity maps and soot-foils were compared against the cell widths from the TPT. It was found that the average error of the cell widths between the TPT and other two measurements were both less than 7.5 %. Additionally, it was found the standard deviation of the cell width measurements were less than 4 mm for each of the measurement techniques, which further shows accuracy when calculating cell widths. The velocity map's cell widths had a lower error compared to the soot-foil's error. This makes sense, as the velocity map can capture finer features than the soot-foil can. The shadowgraph footage used to generate the velocity map can also be used to explore transient detonation structures, including Mach stems, transverse waves, incident shocks, and unburnt gas pockets. Additionally, through further data processing, information for temperature, pressure, and density can be obtained. While these benefits are numerous, it is important to note that the velocity map was made possible by narrowing the channel significantly, which will undoubtedly introduce wall effects. This is important to note when calculating detonation characteristics.

Finally, the cell widths obtained experimentally from the triple point tracks were compared to the Detonation Database, which showed good agreement, and further supports that as the nitrogen dilution increases, the cell width also increases. Cell widths could not be accurately measured above 20 % nitrogen dilution, as the cell widths became too large to view.

Overall, velocity maps can capture more data than soot-foils but are confined to working in a flow where there is heavy influence from the wall.

6 References

[1] Shepherd, J., Pintgen, F., Austin, J., & Eckett, C. (2002, January 14). The structure of the detonation front in gases. *40th AIAA Aerospace Sciences Meeting & Exhibit*. 40th AIAA Aerospace Sciences Meeting & Exhibit, Reno, NV, U.S.A. https://doi.org/10.2514/6.2002-773

[2] Alicherif, M., Rojas Chavez, S. B., Chatelain, K. P., Guiberti, T. F., & Lacoste, D. A. (2024). Experimental characterization of the cell cycle for multicellular detonations. *Combustion and Flame*, *266*, 113553. https://doi.org/10.1016/j.combustflame.2024.113553

[3] Shepherd, J. E., Moen, I. O., Murray, S. B., & Thibault, P. A. (1988). Analyses of the cellular structure of detonations. *Symposium (International) on Combustion*, *21*(1), 1649–1658. https://doi.org/10.1016/S0082-0784(88)80398-9

[4] Zhang, B., Liu, H., & Yan, B. (2019). Investigation on the detonation propagation limit criterion for methane-oxygen mixtures in tubes with different scales. *Fuel*, *239*, 617–622. https://doi.org/10.1016/j.fuel.2018.11.062

[5] R. Akbar, M.J. Kaneshige, E. Schultz, and J.E. Shepherd. Detonations in H_*2*-N_*2*O-CH_*4*-NH_*3*-O_*2*-N_*2* mixtures. Technical Report FM97-3, Explosion Dynamics Laboratory, California Institute of Technology, 1997.

[6] Frederick, M. D., Gejji, R. M., Shepherd, J. E., & Slabaugh, C. D. (2023). Statistical analysis of detonation wave structure. *Proceedings of the Combustion Institute*, *39*(3), 2847–2854. https://doi.org/10.1016/j.proci.2022.08.054

[7] Berson, J., Cideme, R., Brown, T. Hytovick, R., Ahmed, K. (2024, January 4). Statistical Variability of Quasi-2D Hydrocarbon Detonations. *AIAA SCITECH 2024 Forum.* AIAA SCITECH 2024 Forum, Orlando, FL. https://doi.org/10.2514/6.2024-2785

[8] Berson, J., Cideme, R., Hytovick, R., & Ahmed, K. A. (2025, January 6). Pressure Field Variations in Near-Limit Gaseous Detonations. *AIAA SCITECH 2025 Forum*. AIAA SCITECH 2025 Forum, Orlando, FL. https://doi.org/10.2514/6.2025-1963

[9] Pintgen, F., & Shepherd, J. E. (2009). Simultaneous Soot Foil and PLIF Imaging of Propagating Detonations. *19th International Colloquium on the Dynamics of Explosions and Reactive Systems*

[10] Carter, M., & Blunck, D. L. (2022). Direct Comparison of Schlieren and Soot Foil Measurements of Detonation Cell Sizes. *Frontiers in Aerospace Engineering*, *1*, 892330. https://doi.org/10.3389/fpace.2022.892330

[11] Hargather, M. J., & Settles, G. S. (2010). Natural-background-oriented schlieren imaging. *Experiments in Fluids*, *48*(1), 59–68. https://doi.org/10.1007/s00348-009-0709-3